IOP Publishing Journal of Physics: Condensed Matter
J. Phys.: Condens. Matter **32** (2020) 285503 (5pp) https://doi.org/10.1088/1361-648X/ab7fdb

Intrinsic defects of GaSe

Peter Deák[1,5], Miaomiao Han[2], Michael Lorke[1], Meisam Farzalipour Tabriz[1,3] and Thomas Frauenheim[1,4]

[1] Bremen Center for Computational Materials Sci., University of Bremen, PoB 330440, D-28334 Bremen, Germany
[2] Key Laboratory of Materials Physics, Institute of Solid State Physics, Chinese Academy of Sciences, Hefei 230031, People's Republic of China
[3] Max Planck Computing and Data Facility, Gießenbachstr. 2, D-85748 Garching, Germany
[4] Computational Science Research Center (CSRC) Beijing and Computational Science and Applied Research (CSAR) Institute Shenzhen, No.10 East Xibeiwang Road, Haidian District, Beijing 100193, People's Republic of China

E-mail: deak@bccms.uni-bremen.de

Received 7 January 2020, revised 3 March 2020
Accepted for publication 13 March 2020
Published 15 April 2020

Abstract

GaSe is a layered semiconductor with an optical band gap tunable by the number of layers in a thin film. This is promising for application in micro/optoelectronics and photovoltaics. However, for that, knowledge about the intrinsic defects are needed, since they may influence device behavior. Here we present a comprehensive study of intrinsic point defects in both bulk and monolayer (ML) GaSe, using an optimized hybrid functional which reproduces the band gap and is Koopmans' compliant. Formation energies and charge transition levels are calculated, the latter in good agreement with available experimental data. We find that the only intrinsic donor is the interlayer gallium interstitial, which is absent in the case of the ML. The vacancies are acceptors, the selenium interstitial is electrically inactive, and small intrinsic defect complexes have formation energies too high to play a role in the electronic properties of samples grown under quasi-equilibrium conditions. Bulk GaSe is well compensated by the intrinsic defects, and is an ideal substrate. The ML is intrinsically p-type, and p-type doping cannot be compensated either. The opening of the band gap changes the defect physics considerably with respect to the bulk.

Keywords: GaSe, 2D-materials, intrinsic defects, hybrid functional

(Some figures may appear in colour only in the online journal)

1. Introduction

GaSe, a layered semiconductor with a structure similar to MoS_2 (Mo replaced by a pair of Ga-atoms oriented normal to the planes), is often used in non-linear optics [1] and for the generation and detection of electromagnetic waves [2, 3]. In monolayer (ML) form it can also exhibit exotic properties like giant piezoelectricity [4] or tunable magnetism [5], and the possibility of tuning the optical gap of thin films by the layer thickness, between 2 and 3.5 eV [6, 7], opens up the way to further applications in photovoltaics and electronics [8]. Defect engineering is a critical part of any device technology, and it is based on the knowledge about the electronic properties of the most common defects. Obviously, establishment of such a database should start with the intrinsic point defects. From experiments, data on electronic transitions are available for both undoped (e.g. references [9–11]) and doped (e.g. references [12–16]) samples, however the assignment of these to particular intrinsic defects has been, at best, tentative. In particular, it is speculated that an acceptor level about 0.2 eV above the valence band edge (E_V) at room temperature (RT) [10, 15], which moves to $E_V + 0.1$ eV below 200 K [9, 11], can be assigned to the gallium vacancy (V_{Ga}), while a level about 0.2 eV below the conduction band edge (E_C) to the gallium interstitial (Ga_i) [11]. Theory can help the assignment by calculating the electronic transitions, however, calculations for the defects of GaSe, carried out in the local density approximation (LDA) [16] or in the semi-local generalized gradient

[5] Author to whom any correspondence should be addressed.

approximation (GGA) [17, 18] to density functional theory (DFT), suffer from the uncertainties arising from the underestimation of the band gap. Recently, this problem is being circumvented by the use of semi-empirical hybrid functionals [19], but in GaSe we are aware only of one such defect study on As-doping [20]. Therefore, in this paper we report a comprehensive study of the intrinsic defects of both bulk and ML-GaSe, using a Heyd–Scuseria–Ernzerhof (HSE) functional, tuned to comply with the generalized Koopmans' theorem and to simultaneously reproduce the relative position of the band edge states over the entire Brillouin zone [21]. The intrinsic charge transitions levels observed so far can well be explained based on our results. We find that undoped bulk GaSe is a compensated semi-insulator under any stoichiometry (assuming quasi-eqilibrium growth conditions), and the intrinsic defects can also compensate both n- and p-type doping. This is not the case in the ML though, which is weakly p-type if undoped, and p-type doping cannot be compensated either. In section 2 we describe the theoretical framework, while sections 3 and 4 contain our results for the bulk and for the ML, respectively. Finally we conclude in section 5.

2. Computational framework

Our calculations have been carried out with the Vienna *ab initio* simulation package, VASP 5.4.4, using the projector augmented wave method [22]. A 320 (640) eV cutoff was applied for the expansion of the wave functions (charge density). A test with 420 (840) eV has shown negligible difference in the band structure. The semi-core Ga 3d states were not considered explicitly. While these states play a role for interstitial defects in Ga_2O_3, [23] their inclusion in GaSe did not change our results for Ga_i appreciably. Van der Waals interactions between the layers of the bulk crystal were taken into account by the Tkatchenko–Scheffler method [24], using $s_R = 0.96$. The equilibrium geometry was determined for the primitive unit cell with a Γ-centered $6 \times 6 \times 2$ Monkhorst–Pack (MP) k-point set [25], based on constant volume relaxations and fitting to Murnaghan's equation of state [26], resulting in the lattice parameters $a = 3.737$ Å and $c = 15.913$ Å, in close agreement with the experimental values, $a = 3.743$ Å and $c = 15.920$ Å, respectively [27]. Defect calculations in the bulk have been carried out in an orthogonal supercell of 192 atoms (with lattice vectors $4\mathbf{a}_1$, $3\mathbf{a}_1+6\mathbf{a}_2$, $\mathbf{a}_3$, where $\mathbf{a}_i$ are the primitive unit vectors), using the Γ-point approximation. (At present, this is the biggest affordable size). Geometries were relaxed at fixed lattice constants in the supercell, using a force criterion of 0.02 eV $Å^{-1}$. In calculations for the monolayers, the interlayer separation was increased to 25 Å.

The total energy of charged defects was corrected *a posteriori* for the artificial interaction between the repeated charges, using the SLABCC code [28, 29]. SLABCC realizes the Komsa–Pasquarello method [30, 31] to calculate the total energy correction, and can be used for orthogonal supercells of the bulk, slabs and monolayers alike. From the viewpoint of the last two, it is especially important that it allows the use of non-spherical and/or multiple Gaussian models of the defect charge, as well as an anisotropic dielectric constant in the solid part. The charge correction requires the dielectric constant of the material. In principle, for frozen geometry (vertical ionization) the high frequency dielectric constant, ε_∞, while for the optimized geometry (adiabatic ionization) the static dielectric constant, ε_0, is relevant. Earlier, however, we have observed that using ε_∞ also for adiabatic ionization reproduces the experimental values of the charge transition levels better [23, 32, 33]. The explanation probably is that relatively large supercells describe a substantial part of the ionic screening explicitly, and using the bulk value of ε_0 amounts to double-counting. Surprisingly, the dielectric tensor of layered bulk GaSe is quite isotropic, but the experimental values [34–36] show some variation. Therefore, we have used the directional average of the calculated values ($\varepsilon^{\infty}{}_{\perp} = 6.30$, $\varepsilon^{\infty}{}_{||} = 5.62$ eV), [21] i.e., 5.95, for the charge correction. Using the method of Noh *et al* [37], the calculation for the ML resulted in a surprisingly small change ($\varepsilon^{\infty}{}_{\perp} = 6.44$, $\varepsilon^{\infty}{}_{||} = 5.31$ eV), the average being 5.85 [21].

The crucial part of theoretical defect studies using DFT is the choice of the exchange functional. As shown before, quantitatively accurate electronic transitions can only be obtained if the calculated total energy, as function of the occupation numbers, shows the proper piecewise linear behavior [38–40]. The mixing parameter α and the screening parameter μ of an HSE(α,μ) functional can be tuned to achieve that (unless the screening is strongly orbital dependent) [23], and such optimized functionals provided highly accurate defect results in group-IV semiconductors [41], in the polymorphs of TiO_2 [42], and in various Ga-based materials [40]. Layered bulk GaSe has a rather uniform electron distribution, the electron density in the interlayer region being similar to that between the structural units of the layer. (As a consequence the anisotropy of the dielectric constant is relatively small, as shown above.) This has allowed to find an optimized hybrid, HSE(0.40,0.25), which reproduces the band gap and is Koopmans-compliant for bulk GaSe [21]. The interface with vacuum in the case of ML-GaSe, however, has a big influence inside the layer as well, as the electronic screening is weakened. Therefore, the effect of the Hartree–Fock type exchange in the hybrid functional increases, corresponding to a longer screening length (smaller screening parameter) and higher ratio of the non-local exchange. As described in reference [21] in detail, the parameters had to be retuned for the monolayer, where the optimal Koopmans compliant hybrid, which also reproduces the gap, is HSE(0.50,0.10).

As mentioned above, HSE(0.40,0.25) provides highly accurate structural data for bulk GaSe. The resulting single particle band gap (at 0 K) is 2.26 eV. For comparison, the experimental optical band gap is 2.02 eV at RT [1] and 2.13 eV at 4 K [43], while the single particle band gap must be even wider than that, due to electron–phonon renormalization [44]. We have also tested the performance of HSE(0.40,0.25) on charge transition levels. Resistivity, Hall-effect, and TSC (thermally stimulated current) measurements at RT for the substitutional donors Si_{Ga}, Ge_{Ga}, and Sn_{Ga} result in (+/0) charge transition levels around $E_C - 0.6$ eV [12, 14]. For these donors we obtain values at ∼0.7 eV below E_C. Considering the 0.23 eV difference between our 0 K single particle gap and the RT optical

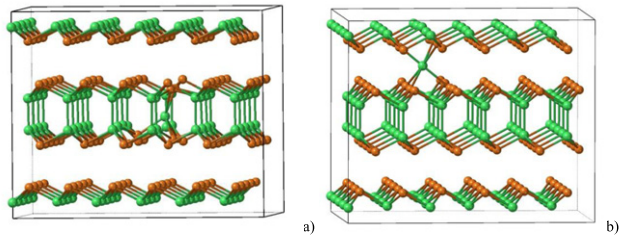

Figure 1. Equilibrium geometry of V_{Ga} and Ga_i in bulk GaSe. (Green and ochre spheres are Ga and Se atoms, respectively.)

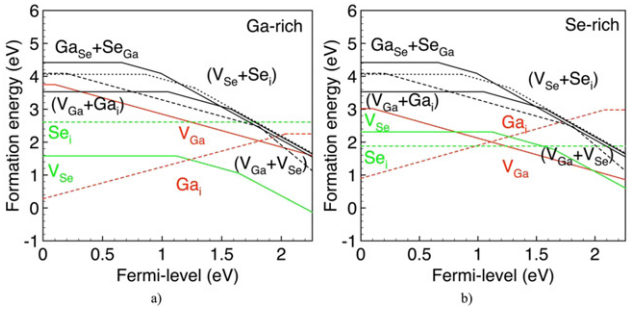

Figure 2. Formation energy (eV) of the intrinsic defects in bulk layered GaSe for various position of the Fermi-level (E_F) in the gap, calculated for extreme Ga-rich (a) and Se-rich (b) conditions. Only the charge state with lowest energy is shown at each E_F. The tangent of the lines, 0, ±1, and ±2, correspond to the charge state.

gap, the calculated charge transition levels should be about 0.12 eV deeper than seen in RT experiments (assuming a symmetric opening of the gap with temperature), which is indeed the case.

The HSE(0.50,0.10) hybrid provides 4.43 eV as the single particle band gap of ML-GaS at 0 K. This agrees well with the result of a GW_0 calculation, 4.38 eV [21], but it is considerably wider than photoluminescence (PL) data reported for the ML, ∼3.4 eV [45]. It is well known, however, that the exciton binding energy is very high in monolayers, because of geometric confinement [46] and reduced dielectric screening [47], so the single particle band gap must be wider (by about 1 eV) than the exciton recombination energy measured in PL.

Finally we note that the standard HSE06 hybrid strongly underestimates the gap both in the bulk and in the ML, and is not Koopmans' compliant either.

3. Results for the bulk

We have calculated the vacancies (V_{Ga}, V_{Se}), the interstitials (Ga_i, Se_i), the first-neighbor Frenkel pairs ($V_{Ga}Ga_i$ and $V_{Se}Se_i$), the antisite pair ($Ga_{Se}Se_{Ga}$) and the divacancy ($V_{Ga}V_{Se}$) in all their charge states which are stable in the Fermi-level range between E_V and E_C. While V_{Se} shows only a relatively small rearrangement of the neighboring atoms (the Ga-atoms moving towards each other), the global energy minimum for V_{Ga} is a 'split vacancy', where the pair of the missing Ga atom moves toward the middle of the layer, forming 5 bonds to nearby Se atoms with bond lengths of 2.54, 2.58, 2.58, 2.73, 2.73 Å (figure 1(a)). A similar structure was found and experimentally confirmed by scanning tunneling microscopy recently [48]. The equilibrium position of Se_i is a puckered bond-center interstitial between a pair of Ga atoms, while Ga_i occupies preferentially an octahedral interstitial site between two layers (figure 2(b)).

Figure 2 shows the formation energy of the intrinsic defects as a function of the Fermi-level position in the band gap. Using the method described in reference [38], these have been calculated for the extreme Ga-rich case, assuming metallic Ga as the reservoir for Ga atoms (as described in reference [33]), and for the extreme Se-rich case, assuming Ga_2Se_3 to be the reservoir for Se.

V_{Ga} has an effective-mass-like delocalized acceptor state. The (0/−) charge transition level is calculated to be at E_V + 0.1 eV, equal to the low temperature (<200 K) experimental value of reference [9], and is also in line with low temperature PL measurements [49]. In contrast, Ga_i is a donor, with the (+/0) charge transition level calculated at $E_C - 0.2$ eV, again in good agreement with experiment [11]. V_{Se} is a deep double acceptor, with the first ionization level at midgap. Se_i is electrically inactive (with two lone pairs on the extra Se atom, the energy level of which being deep in the valence band).

In the extreme Ga-rich limit, the lowest energy intrinsic defect under n-type conditions is the double acceptor V_{Se}, while under p-type conditions the Ga_i donor. Under extreme Se-rich conditions the situation is similar but V_{Ga} may also play a role in n-type samples. All of these defects are acting as compensating centers.

The calculated complexes are all deep double acceptors, with relatively high formation energy, which is, however, still lower in each case than the sum of the formation energies of the constituents. In principle, such complexes may, therefore, be formed upon annealing, provided the diffusion barrier is sufficiently low. This is more likely for the interstitials, so we calculated their energy halfway between the minimum positions to give an estimate. For Se_i the diffusion barrier is higher than 3 eV, for Ga_i it is about 1 eV. Therefore, only the latter is expected to be mobile, as observed for adatoms between the layers [48]. This means that $V_{Ga}Ga_i$ complexes may easily form. The charge transition levels of this deep double acceptor happen to nearly coincide with those of V_{Se}.

In order to establish the electronic behavior of undoped samples, the self-consistent calculation of the Fermi-level and the relative abundance of the individual intrinsic defects are required, using the neutrality condition

$$N_C \exp\left(-\frac{E_C - E_F}{kT}\right) + \sum_i |q_i|\,(N_{Ai} - p_{Ai}) = N_V \exp\left(-\frac{E_F - E_V}{kT}\right) + \sum_i |q_i|\,(N_{Di} - n_{Di}) \quad (1)$$

where N_{Di}, N_{Ai} are the concentrations of the various donor and acceptor defects, respectively, as determined by their formation energy. N_C, N_V are the effective densities of states at E_C and E_V, respectively, and n_{Di}, p_{Ai} are the concentration of

electrons on the donor and holes on the acceptor levels, respectively. Details can be found, e.g., in reference [50]. To solve equation (1), the code of Buckeridge was used [51]. To calculate N_C and N_V, we have used the density-of-states effective masses, 0.73 m_e for electrons and 2.44 m_e for holes [17]. The temperature was set to 1000 °C, which is typical in the single crystal growth of bulk GaSe.

Taking all the calculated intrinsic defects into account, the most abundant defects are, as expected, Ga_i with concentrations of $\sim 6 \times 10^{16}$ cm^{-3} under Ga-rich, and $\sim 2 \times 10^{14}$ cm^{-3} under Se-rich conditions, and V_{Se} with $\sim 3 \times 10^{16}$ cm^{-3}, and $\sim 2 \times 10^{14}$ cm^{-3}, respectively. That means almost perfect compensation, with the Fermi-energy being at $E_V + 1.16$ eV under Ga-rich, and at $E_V + 1.03$ eV under Se-rich conditions, i.e., slightly above and below midgap ($E_V + 1.13$ eV). The intrinsic carrier concentration is only 1.5×10^{16} cm^{-3} even at 1000 °C, so undoped bulk GaSe, grown under any stoichiometric condition, is a fairly good semi-insulator. If n- or p-type conductivity is observed in as-grown samples, they must be unintentionally doped (or not in equilibrium). The low formation energies of Ga_i and V_{Se} also mean that intentional doping will also be compensated. It should be noted, however, that Ga_i has a low diffusion barrier in the channel between the layer and might be annealed out.

As mentioned above, the acceptor level of V_{Ga} and the donor level of Ga_i, predicted here, has been observed experimentally. The other dominant defect is V_{Se}, having (hyper) deep acceptor levels at $E_V + 1.1$ eV and $E_V + 1.6$ eV for the charge transitions (0/–) and (–/2–), respectively, so it acts as a double electron trap. To our knowledge, these levels have not been yet observed, probably because the midgap region is dominated by extended defects [10, 49].

4. Results for the monolayer

The defect physics changes markedly in the ML, with respect to the bulk case. First of all, although the structure of V_{Ga}, V_{Se}, and Se_i does not change much, in absence of a neighboring layer, Ga_i becomes a high energy defect which cannot play a role in the electronic properties. Therefore, there is no intrinsic donor defect to compensate p-type doping. Secondly, the larger gap in the ML changes the observable charge transition levels of the vacancies (see figure 3).

As mentioned before, the single particle gap of the ML increases to 4.43 eV at 0 K (from 2.26 eV in the bulk) [21], due to the lack of both Van der Waals and covalent interactions between the layers [7]. Since the gap states of V_{Se} are formed by Ga orbitals, its charge transition levels move up with E_C (which is dominated by Ga states), and the (2-) charge state is not stable anymore. The retreating E_V reveals the localized states of V_{Ga} (composed of Se-orbitals). The (0/-) level becomes deep and a (+/0) level appears above E_V. Since V_{Ga} has a high formation energy (except for n-type samples grown under extreme Se-rich conditions) and Se_i is again electrically inactive, the (0/–) charge transition level of V_{Se} will pin the Fermi-level at 3.3 eV above E_V. The complexes mentioned in the bulk do not play a significant role in the ML either. It should be noted though, that chalcogenide vacancies get easily

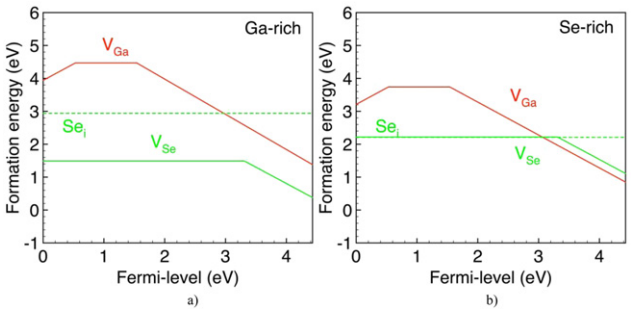

Figure 3. Formation energy (eV) of the intrinsic defects in ML-GaSe for various position of the Fermi-level E_F in the gap, calculated for extreme Ga-rich (a) and Se-rich (b) conditions.

filled by oxygen or other foreign atom in case of monolayers [52, 53]. Investigations of such substitutional impurities are, however, beyond the scope of this paper.

In lack of the interlayer Ga_i defects, p-type doping will not be compensated, while the vacancies still can compensate n-type doping. Therefore, ML-GaSe can be easily doped p-type, in accordance with experience [8], while n-type doping will be difficult.

5. Summary

We have carried out a comprehensive study of the basic point defects and their pairs in both bulk and ML-GaSe, using an optimized hybrid functional, which is Koopmans' compliant and reproduces the low temperature single particle band gap. Such a functional allows the accurate calculation of charge transition levels. We have identified the gallium vacancy as source of the intrinsic acceptor level 0.2 eV above the valence band edge, observed at room temperature, and the gallium vacancy as the intrinsic donor with a level 0.2 eV below the conduction band. The selenium vacancy was found to be a deep double acceptor with charge transition levels 1.1 and 1.6 eV above E_V, while the selenium interstitial was found to be electrically inactive. Pairs of these defects do not play a role in the electronic properties under equilibrium conditions. We have found that undoped bulk samples in equilibrium are well compensated under any stoichiometry, with a low concentration of free carriers up to 1000 °C. The intrinsic defects can also compensate both n- and p-type doping in the bulk. This makes GaSe an ideal substrate for monolayer semiconductors. The opening of the gap in few-layer GaSe changes the defect physics, and the absence of low energy interlayer Ga_i makes ML-GaSe intrinsically p-type due to the vacancies. In lack of low energy donor-type intrinsic defects, p-type doping is not compensated in the ML either, while n-type doping might be difficult.

Acknowledgments

Funding by the DFG research project FR2833/63–1, and the support of the Supercomputer Center of Northern Germany (HLRN Grant No. hbc00027), as well as of the National

Natural Science Foundation of China under Grant No. 61804154 is acknowledged.

ORCID iDs

Peter Deák https://orcid.org/0000-0003-4839-7345

References

[1] Allakhverdiev K R, Yetis Ö M, Özbek S, Baykara T K and Salaev E Y 2009 *Laser Phys.* **19** 1092
[2] Liu K, Xu J and Zhang X-C 2004 *Appl. Phys. Lett.* **85** 863
[3] Shi W, Ding Y J, Mu X and Fernelius N 2002 *Appl. Phys. Lett.* **80** 3889
[4] Fei R, Li W, Li J and Yang L 2015 *Appl. Phys. Lett.* **107** 173104
[5] Cao T, Li Z and Louie S G 2015 *Phys. Rev. Lett.* **114** 236602
[6] Rybovskiy D V *et al* 2011 *Phys. Rev.* B **84** 085314
[7] Lei S *et al* 2013 *Nano Lett.* **13** 2777
[8] Late D J, Liu B, Luo J, Yan A, Ramakrishna Matte H S S, Grayson M, Rao C N R and Dravid V P 2012 *Adv. Mater.* **24** 3549
[9] Tatsuyama C, Hamaguchi C, Tomita H and Nakai J 1971 *Jpn. J. Appl. Phys.* **10** 1698
[10] Micocci G, Siciliano P and Tepore A 1990 *J. Appl. Phys.* **67** 6581
[11] Shigetomi S and Ikari T 2003 *J. Appl. Phys.* **94** 5399
[12] Micocci G, Serra A and Tepore A 1997 *Phys. Status Solidi* (*a*) **162** 649
[13] Sánchez-Royo J F, Errandonea D, Segura A, Roa L and Chevy A 1998 *J. Appl. Phys.* **83** 4750
[14] Shigetomi S and Ikari T 2005 *Jpn. J. Appl. Phys.* **44** 7521
[15] Cui Y, Dupere R, Burger A, Johnstone D, Mandal K C and Payne S A 2008 *J. Appl. Phys.* **103** 013710
[16] Huang C, Wang Z, Ni Y, Wu H and Chen S 2017 *RSC Adv.* **7** 23486
[17] Rak Z, Mahanti S D, Mandal K C and Fernelius N C 2009 *J. Phys. Chem. Solids* **70** 344
[18] Chen H, Li Y, Huang L and Li J 2015 *RSC Adv.* **5** 50883
[19] Demirci S, Avazh N, Durgun E and Cahangirov S 2017 *Phys. Rev.* B **95** 115409
[20] Bahuguna B P, Saini L K, Sharma R O and Tiwari B 2017 *Comput. Mater. Sci.* **139** 31
[21] Deák P, Khorasani E, Lorke M, Farzalipour-Tabriz M, Aradi B and Frauenheim T 2019 *Phys. Rev.* B **100** 235304
[22] Kresse G and Hafner J 1994 *Phys. Rev.* B **49** 14251
Kresse G and Furthmüller J 1996 *Phys. Rev.* B **54** 11169
Kresse G and Joubert D 1999 *Phys. Rev.* B **59** 1758
[23] Deák P, Duy Ho Q, Seemann F, Aradi B, Lorke M and Frauenheim T 2017 *Phys. Rev.* B **95** 075208
[24] Tkatchenko A and Scheffler M 2009 *Phys. Rev. Lett.* **102** 073005
[25] Monkhorst H J and Pack J K 1976 *Phys. Rev.* B **13** 5188
[26] Murnaghan F D 1944 *Proc. Natl. Acad. Sci. USA* **30** 244
[27] Cenzual K, Gelato L M, Penzo M and Parthé E 1991 *Acta Crystallogr. Sect. B Struct. Sci.* **47** 433
[28] Farzalipour Tabriz M, Aradi B, Frauenheim T and Deák P 2019 *Comput. Phys. Commun.* **240** 101
[29] Farzalipour Tabriz M 2019 Source code https://github.com/MFTabriz/slabcc
[30] Komsa H-P and Pasquarello A 2013 *Phys. Rev. Lett.* **110** 095505
[31] Komsa H-P, Berseneva N, Krashennikov A V and Nieminen R 2014 *Phys. Rev.* X **4** 031044
Komsa H-P, Berseneva N, Krashennikov A V and Nieminen R 2018 *Phys. Rev.* X **8** 039902(E) (Errata)
[32] Deák P, Aradi B and Frauenheim T 2012 *Phys. Rev.* B **86** 195206
[33] Deák P, Lorke M, Aradi B and Frauenheim T 2019 *Phys. Rev.* B **99** 085206
[34] Leung P C, Andermann G, Spitzer W G and Mead C A 1966 *J. Phys. Chem. Solids* **27** 849
[35] Madelung O ed 1996 *Semiconductors: Basic Data* 2nd edn (Berlin: Springer)
[36] Tatsuyama C, Hamaguchi C, Tomita H and Nakai J 1971 *Jap. J. Appl. Phys.* **10** 1698
[37] Noh J-Y, Kim H and Kim Y-S 2014 *Phys. Rev.* B **89** 205417
[38] Freysoldt C, Grabowski B, Hickel T, Neugebauer J, Kresse G, Janotti A and Van de Walle C G 2014 *Rev. Mod. Phys.* **86** 253
[39] Deák P 2018 *Physica* B **535** 35
[40] Deák P, Lorke M, Aradi B and Frauenheim T 2019 *J. Appl. Phys.* **126** 130901
[41] Deák P, Aradi B, Frauenheim T, Janzén E and Gali A 2010 *Phys. Rev.* B **81** 15203
[42] Deák P, Aradi B and Frauenheim T 2011 *Phys. Rev.* B **83** 155207
[43] Maschke K and Levy F 1983 *Landolt-Börnstein in Numerical Data and Functional Relationships in Science and Technology, New Series, Group III: Crystal and Solid State Physics* ed S Flügge (Berlin: Springer)
[44] Cardona M and Thewalt M L W 2005 *Rev. Mod. Phys.* **77** 1173
[45] ChJung S, Shojaei F, Park K, Oh J Y, Im H S, Jang D M, Park J and Kang H S 2015 *ACS Nano* **9** 9585
[46] Li L H *et al* 2015 *Nano Lett.* **15** 218
[47] Hüser F, Olsen T and Thygesen K S 2013 *Phys. Rev.* B **88** 245309
[48] Hopkinson D G *et al* 2019 *ACS Nano* **13** 5112
[49] Capozzi V and Montagna M 1989 *Phys. Rev.* B **40** 3182
[50] Deák P, Gali A, Aradi B, Kaviani M, Frauenheim T and Gali A 2014 *Phys. Rev.* B **89** 075203
[51] Buckeridge J 2018 *SC-Fermi* https://github.com/jbuckeridge/sc-fermi
[52] Giannazzo F *et al* 2017 *ACS Appl. Mater. Interfaces* **9** 23164
[53] Zhu H *et al* 2016 *ACS Appl. Mater. Interfaces* **8** 19119